ZIBELINE INTERNATIONAL™ PUBLISHING

E-ISSN: 2976-2421 (Online)
CODEN: JRAOCQ

JOURNAL OF ROCK ART
(JRA)

DOI: http://doi.org/10.7508/jra.01.2024.09.19

CrossMark

REVIEW ARTICLE

WEATHERING DISEASE CHARACTERISTICS AND IMPACT ASSESSMENT OF HELANKOU ROCK ART

Xiaotong Huo[1,2], Rong Ma[3], Yamin Xiong [1], Erna Ma [4], Jinhua Wang[1*]

[1]Department of Cultural Heritage and Museology at Fudan University, 220 Han-dan Road, Shanghai, 200433, China

[2]Shaanxi History Museum, 91 Xiaozhai East Road, Xi an, 710061, China

[3] Henan Provincal Institute of Cultural Heritage and Archaeology, Zhengzhou 450000, China

[4]Erna Ma, Yinchuan Municipal Administration of Helan Mountain Rock Art, 199 East Square Road, Yinchuan 750001, Ningxia, China,

[*]*Corresponding author Email: jinhuawang@fudan.edu.cn*

ARTICLE DETAILS

Article History:

Received 5 January 2024
Accepted 10 February 2024
Available online 15 March 2024

ABSTRACT

This study investigated the distribution and types of surface weathering diseases on rock art in the Helankou area, using field surveys and statistical analyses. In addition, a damage index analysis method was proposed to quantify the effect of weathering diseases on the integrity and preservation status of the artefacts. The study findings revealed that the weathering diseases affecting the rock art in Helankou primarily encompass surface delamination, splitting, and blistering. Significant variations were observed in the extent of damage to the rock art depending on the rock surface type. Spheroidal surfaces and vertical planes typically exhibit more pronounced damage, whereas parallel planes experience a relatively lower impact. A comparative analysis of the damage indices revealed that the most significant disease affecting the integrity and preservation status of the rock art is delamination, which is predominantly observed on the surfaces of spheroidal weathering planes. This study will facilitate the development of protective measures for paintings. This will lead to improved management strategies and the implementation of measures tailored to different levels of weathering severity.

KEYWORDS

Disease distribution patterns, Damage index, Correlation analysis

1. INTRODUCTION

A prime example of northern Chinese rock art is the rock art located at the eastern foothills of Helan Mountain in Helan County, Yinchuan City, Ningxia Hui Autonomous Region. This rock art, mostly densely concentrated in Helankou, exhibits various forms, such as human faces, animals, and sun gods. They span the Stone Age to the Spring and Autumn, Warring States, and Western Xia dynasties, reflecting the ancient natural ecology of Helan Mountain and the social structure and customs of the inhabitants (He, J.D, 2017).

Owing to the natural surroundings and geological agents, the rock art in Helankou faces potential threats to its integrity and long-term preservation. To implement protective measures for rock art, the preservation status of the art must be thoroughly comprehended and assessed. Stone immovable cultural heritage artefacts typically experience deterioration across three categories: structural instability, infiltration erosion, and rock weathering diseases. Surface weathering challenges are prominent in Helankou rock art. Currently, there is a dearth of extensive studies on the various types, distribution patterns, and severity of weathering diseases that affect Helankou rock art. Thus, it is imperative to conduct a scientific and accurate assessment of this topic to aid conservation decisions and plans for Helankou rock art.

To assess the surface weathering diseases of stone cultural heritage artefacts, these phenomena must be diagnosed and quantitatively described. To achieve this, an internationally recognised set of globally applicable definitions and terms has been established to describe the morphological changes that occur on rock surfaces during weathering (H, Siedel, 2014). In 1979, Arnold et al. proposed the "Terminology of Building Stone Weathering Phenomena" (Arnold A, 1979). In 1995, Fitzner et al. classified the weathering forms of stone cultural artefacts using a tiered structure (Fitzner B, 1995 and J Delgado Rodrigues, 2016). Hongsong proposed an assessment system for the deterioration

Quick Response Code	Access this article online	
	Website www.jora.org.my/	**DOI:** 10.7508/jra.01.2024.09.19

Cite The Article: Xiaotong Huo, Rong Ma, Yamin Xiong , Erna Ma , Jinhua Wang(2024). Weathering disease characteristics and impact assessment of helankou rock art. *Journal of Rock Art*, 3(1): 09-19.

characteristics of stone materials of cultural heritage based on foreign research (Li H.S.,2011 and Zhang J.F., 2007). The "Survey Specification for Stone Cultural Relics Protection Engineering" (WW/T 0063-2015) issued by the State Administration of Cultural Heritage of China in 2015 adopted the aforementioned classification system and established a "Surface Deterioration Damage Classification" system. These standards were established and have been continuously improved to facilitate a better understanding and description of the deterioration phenomena of cultural stone relics, thereby laying the groundwork for in-depth research.

2.DISTRIBUTION OF HELANKOU ROCK ART

According to the natural environment and landform morphology (Fig. 1), rock art in Helankou can be categorised into cliff-wall and prairie rock art distributed across six areas (A, B, C, D, E, and F). Cliff-wall rock art is mainly found in areas B and C, showing composite images with fewer individual images. The gully and its surroundings in the central-eastern part of Helan Mountain had the highest concentrations of these paintings. They are found 1–5 m above ground level, with the highest values not exceeding 20 m.

Based on the geological features and occurrence conditions, the surfaces of rocks that host rock art can be classified into vertical planes, parallel planes, and spheroidal surfaces (Fig. 3). 'Symbol and Human Face Images' in Zone B3 exhibit rock art engraved on irregularly weathered, undulating, and spheroidal surfaces that feature splitting and delamination diseases. The 'Human Face Group' in Zone C4 is the vertical-surface type, whereas the "Human Face and Axe" in Zone C17 is the parallel-surface type. This surface type is characterised by a relatively uniform and flat rock surface.

3.CHARACTERISTICS OF DISEASE TYPES

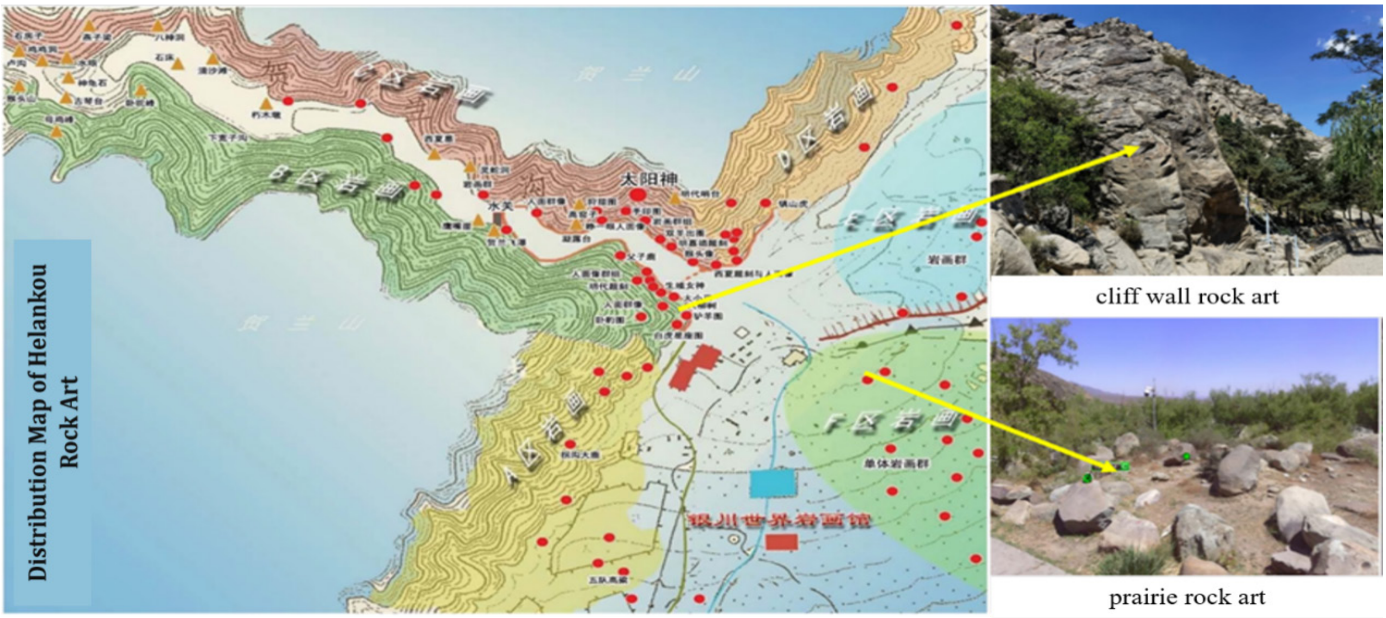

Figure 1: Distribution Map of Helankou Rock Art

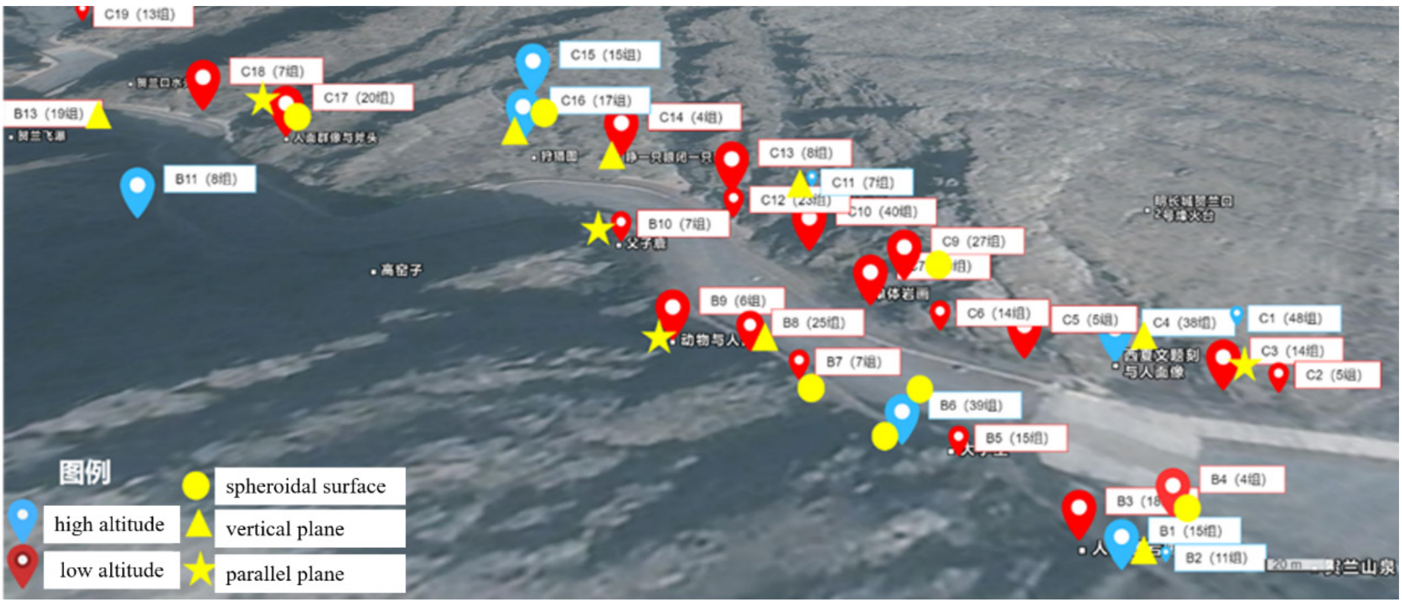

Figure 2: Distribution and Quantity of Rock Art in Zones B and C of Helankou

Fig. 2 shows 14 rock art sites in Zone B (B1–B14), which collectively feature 190 sets of rock paintings. Zone C had 21 rock art sites (C1–C21), including 337 sets of rock paintings. Rock art groups significantly vary in their elevation. Based on the height of the rock paintings from the ground, they are classified into high-altitude (blue) and low-altitude (red) areas. The rock art in low-altitude areas is typically carved on rocks near the ground or in valleys. Contrarily, the rock art in high-altitude areas is primarily engraved on cliffs more than 5 m above ground level.

Spheroidal Surfaces Rock Art (Symbols and Human Faces)

Vertical Plane Rock Art (Human Face Group)

Parallel Plane Rock Art (Human Faces and Axes)

Figure 3: Rock Art Surface Types

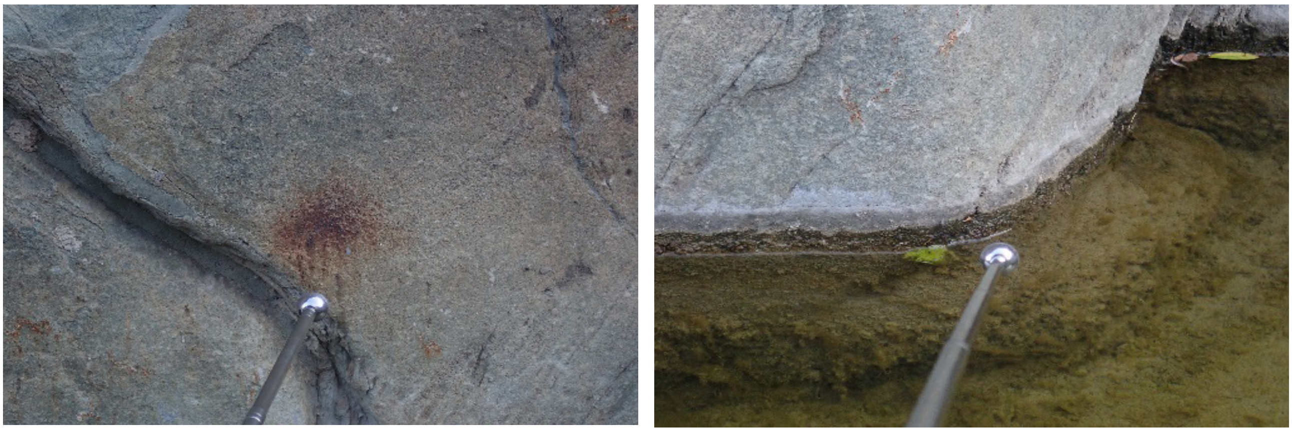

Figure 4: Soiled Surfaces

Table 1: Soiling Statistics

Sample Size	Maximum Value (m^2)	Minimum Value (m^2)	Average Value (m^2)	Standard Deviation
73	7.872	0.001	0.412	1.244

When analysing disease-type characteristics in rock art, it is important to first describe and record the shape of the disease through text and pictures. Next, the disease type is diagnosed. However, identifying on-site diseases can be challenging and is frequently performed using a combination of direct observation and specialised detection equipment. To categorise and grade the existing disease types in the rock art of Helan Mountain, we referred to relevant standard materials and definitions of surface diseases in rocks. After surveying Zones B and C, we identified four major categories of surface diseases: surface rock delamination, blistering, splitting, and soiling. In addition, we conducted a quantitative statistical analysis of the 273 disease maps that were obtained.

Soiling refers to tangible deposits found on stone surfaces. They typically lack adhesion and can be identified based on colour, morphology, size, and origin, if determinable. The deposits on Helankou rock art surfaces primarily comprise dust or musci, which commonly appear yellow or black. Fig. 4 shows that Helankou rock art is contaminated by various substances, such as dust, atmospheric pollution, water rust stains, microbial remnants, and human-induced graffiti and marks. These substances cover rock art surfaces and their surroundings, thereby affecting the expression and value of the art.

This study observed 73 cases of contamination diseases in the area. The most contaminated area spanned 7.827 m^2, located at Zone C4. This particular area of rock art has a relatively large surface that exhibits severe imprints from rubbings and significant coverage by surface water marks. Table 1 presents information on the contamination areas in various samples. The average contaminated area was 0.412 m^2, indicating that most of the samples featured smaller areas affected by contamination, whereas a few outliers had significantly larger areas. The high standard deviation of 1.244 revealed substantial variability around the average value, indicating a significant dispersion among the samples.

Blistering describes a situation in which a particular thickness of the rock surface develops a raised deformation resembling a slab-like structure, resulting in the formation of cavities behind this structure. This is categorised under surface integrity damage, encompassing various types of localised surface damage to cultural heritage rocks that can be repaired under specific conditions. Two types of deformations exist in Helankou rock art. The first type is easily identifiable through direct observation because it causes noticeably raised deformations. The second type is less conspicuous and requires tools, such as an infrared thermal imager and a blistering hammer, for identification. However, the use of an infrared thermal imager on-site requires specific temperature variations. Thus, sunrise and sunset are the most effective times to use it. Oppositely, the use of the blistering hammer involves a gentle slide over the rock art surface to define the affected area. This process results in a noticeable increase in sound frequency in the blistered areas compared with non-blistered areas, rendering it a convenient, straightforward, and efficient identification process (Fig. 5).

Table 2 shows that the survey recorded 109 instances of blistering. The largest blistered area spanned 0.566 m^2, at C14, whereas the smallest spanned 0.01 m^2. The standard deviation for blistering was 0.091, which was quite close to the mean of 0.07. This suggested a tendency for the blistered areas to concentrate around the mean. With a small

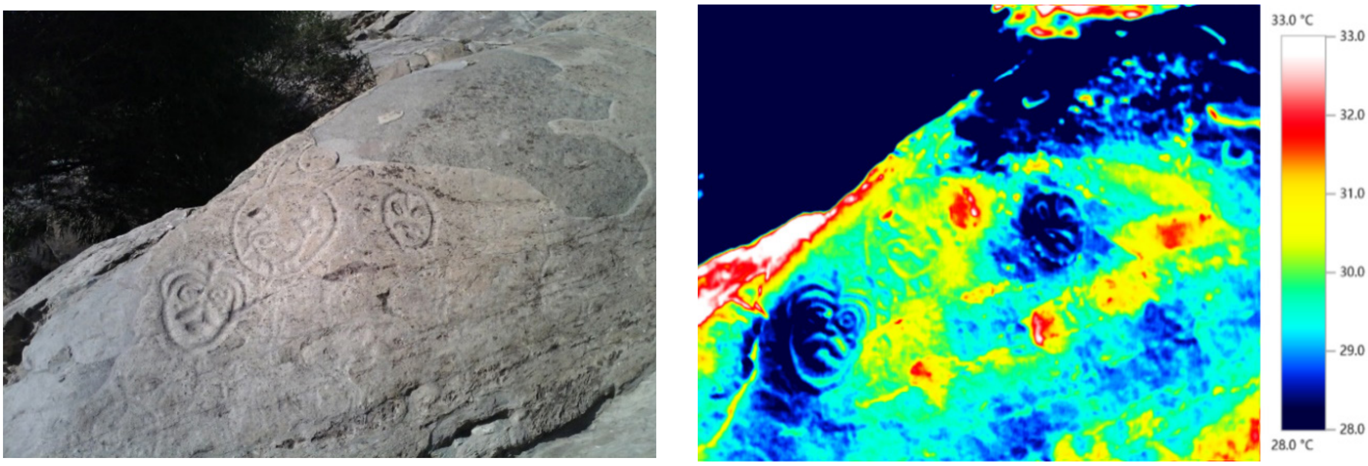

Figure 5: Infrared Thermal Image of blistering

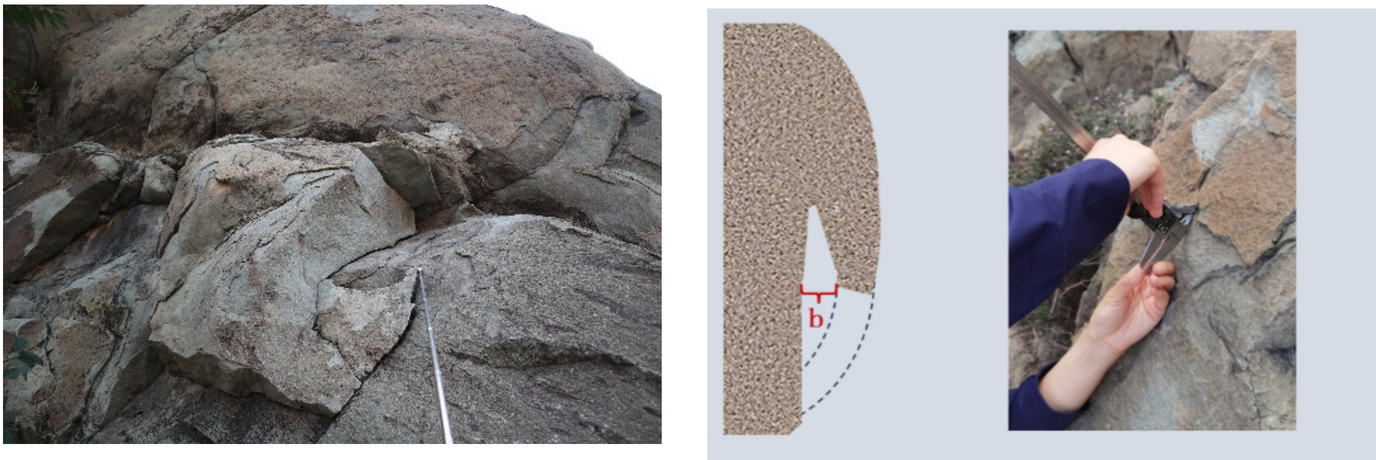

Figure 6: Splitting Image

Figure 7: Delamination Image

standard deviation, the range of variation in the blistered areas was narrow, indicating that most of the blistered areas were close to the average. This may imply a relatively consistent and stable distribution of blistered areas in the sample.

Splitting refers to the phenomenon in which various fissures intersect within the rock art surface, causing the stone to fracture along planes of weakness, such as microcracks or clay, without completely peeling off. Fissures and cracks at different developmental stages contribute to surface integrity damage. For statistical convenience, we merged and tallied the splitting but provided specific markings for different splittings. The geometric form of the splitting damage was measured (Fig. 6), where 'b' represents the width of the split, and the estimated split area was the product of the length and width. The resulting flaking caused by this disease poses a serious threat to the long-term

Table 2: Blistering Statistics

Sample Size	Maximum Value (m^2)	Minimum Value (m^2)	Average Value (m^2)	Standard Deviation
109	0.566	0.002	0.070	0.091

Table 3: Splitting Statistics

Sample Size	Maximum Value (m^2)	Minimum Value (m^2)	Average Value (m^2)	Standard Deviation
187	0.515	0.003	0.097	0.087

Table 4: Delamination Statistics

Sample Size	Maximum Value (m^2)	Minimum Value (m^2)	Average Value (m^2)	Standard Deviation
241	1.725	0.002	0.279	0.35

preservation of the rock art on Helan Mountain rock and is reparable.

Table 3 presents the splitting data based on a relatively large sample size of 187. The largest splitting damage area spanned 0.515 m^2, at C10, and the smallest area spanned 0.003 m^2. A standard deviation of 0.087 indicated that the splitting damage areas were relatively concentrated, with minimal variation in the data.

Detachment refers to the gradual separation of the surface layer of the rock art from the rock mass. It involves physical separation into one or multiple layers of various thicknesses and diverse forms, including detachment and scaling. Helankou rock art mainly exhibits surface delamination (Fig. 7), which is a type of surface damage that significantly impacts the deterioration of cultural stone relics. Without a proper basis, it is usually impossible to repair the surface loss of stone cultural heritage artefacts.

Table 4 shows that detachment was observed in 241 samples with a wide distribution. The detachment significantly varied in the affected areas. A standard deviation of 0.35 suggested a significant degree of variability in the area affected by detachment.

4.DISEASE DISTRIBUTION ANALYSIS

The measurement of the size and configuration of damage on rock art surfaces, such as cracks or discolouration, helps to assess the extent of affected areas, known as the 'ailment coverage rate'. This signifies the proportion of the damaged surface area. This rate provides an understanding of the damage distribution across the rock art surface. Here, the ailment coverage rate was employed to ascertain if the damage was concentrated or dispersed among the different locations and surface types of rock art. If the coverage rate of diseases was low, only a small area of the rock art was affected. This suggests that the rock surface had undergone minimal erosion or damage; therefore, the featured content remained intact, visible, and preserved. Conversely, a high ailment coverage rate indicated a larger affected area, which could imply that the rock art had suffered a significant loss. In severe cases, certain art content may even disappear entirely, leading to the loss of artistic value and important information.

Fisher's exact test is a statistical technique employed to analyse the relationship between two or more categorical variables. It is a non-parametric method that was used to examine the association between the disease coverage rate and the location or surface type of rock art. This method provides a precise description of the disease distribution characteristics.

4.1 Coverage Rate Statistics for Diseases

Using CAD measurements of the area and length of line segments, different disease types were calculated along with the rock art area. Thereafter, the measurements were proportionally converted into the actual ailment area or length of the rock art. The image proportion is the ratio of the area or length of the CAD drawing to the actual area of the rock art. Table 5 lists the coverage rates of diseases in Zones B and C, expressed as a percentage of the disease area to the rock art area, along with their corresponding rock art types.

Fig. 8 shows the detachment coverage rate. Minor detachment diseases occurred in Zones B5, B8, B13, C13, C15, and C16, with coverage rates below 10%. Moderate detachment diseases were observed in zones B1, B2, B4, C3, C4, C5, C6, C7, C8, C9, C11, C14, and C19, with coverage rates in the range of 10%–25%. Severe detachment diseases were observed in Zones B3, B6, B7, B9, C1, C2, C10, C12, and C18, with coverage rates above 25%.

Fig. 9 illustrates the extent of blistering coverage. Minor blistering was observed in Zones B1, B4, B5, B6, B7, B9, B13, C3, C4, C5, C6, C7, C10, C12, C14, C17, C18, and C19, with coverage rates below 5%. Moderately severe blistering was observed in Zones B3, C2, C13, and C16, with coverage rates of 5%–10%. Zones B2, B8, C1, C9, and C15 did not exhibit blistering.

The splitting coverage rate shown in Fig. 10 revealed relatively severe areas where surface cracks were prevalent. These were Zones B1, B2, B4, B5, B6, B13, C1, C2, C5, C7, C10, C12, C13, C18, and C19. In these areas, the splitting coverage rate range was 10%–40%. However, other areas with relatively fewer surface splitting occurrences below 10% were observed.

The soiling coverage rate is shown in Fig. 11. B9, B13, C1, and C2 were the major pollution-affected zones, with ailment coverage rates above 10%. The other zones had relatively fewer disease occurrences (all below 10%).

4.2Correlation Analysis of Disease Distribution

Fisher's exact test in IBM SPSS Statistics was employed to examine the correlation between the diseases observed in Helan Mountain rock art and the elevation and surface types of the rock art locations.

The small-probability event difference test method, developed by British statistician R. A. Fisher (1890–1962), involves representing data in a two-dimensional contingency table. The rows in the table represent different values of one categorical variable, and the columns represent different values of another categorical variable (Fisher R A., 1922). The method calculates the probability (p-value) of observing the given data or more extreme outcomes across all possible data distributions.

If the *p*-value is less than a predetermined significance level (usually 0.05), this indicates a significant correlation between two categorical variables. This method is employed to determine if the numerical data follow a specific distribution pattern and if the impact of the factors differs. This is particularly helpful for small sample sizes, particularly in cases with sparse data, with a sample size below 40. Fisher's exact test is more accurate than the chi-square test; however, it incurs higher computational costs.

Table 5: Statistics of Rock Art Diseases

Number	Detachment Coverage (%)	Blistering Coverage (%)	Splitting Coverage (%)	Soiling Coverage (%)	Location Division	Surface Type
B1	17.55	0.47	25.03	1.06	High	Vertical Plane
B2	20.96	0	14.55	0	High	Parallel Plane
B3	51.49	7.38	0	0	Low	Spheroidal Surface
B4	23.48	1.06	13.92	3.17	Low	Parallel Plane
B5	6.12	2.81	10.92	1.60	Low	Vertical Plane
B6	31.30	1.84	15.18	11.00	High	Spheroidal Surface
B7	31.33	0.23	3.25	2.80	Low	Spheroidal Surface
B8	6.88	0	2.42	0.36	Low	Parallel Plane
B9	38.97	0.75	2.74	10.34	Low	Vertical Plane
B13	4.27	3.60	13.13	14.95	Low	Vertical Plane
C1	28.17	0	34.04	20.42	High	Vertical Plane
C2	30.88	7.41	12.06	25.26	Low	Vertical Plane
C3	16.85	2.75	7.67	4.58	Low	Vertical Plane
C4	11.68	1.70	3.07	9.27	High	Parallel Plane
C5	20.04	2.51	12.59	1.67	Low	Vertical Plane
C6	22.73	3.41	7.52	5.11	Low	Vertical Plane
C7	18.09	3.27	20.53	3.52	Low	Spheroidal Surface
C9	16.62	0	8.31	0.96	High	Spheroidal Surface
C10	36.15	3.25	19.85	2.19	High	Spheroidal Surface
C11	23.08	0	0	4.43	High	Vertical Plane
C12	29.00	2.90	12.17	2.19	Low	Spheroidal Surface
C13	8.25	6.36	15.99	1.19	Low	Vertical Plane
C14	13.63	1.82	1.39	0	High	Vertical Plane
C15	8.80	0	5.04	0	High	Parallel Plane
C16	4.71	11.87	10	0	High	Spheroidal Surface
C17	11.03	0.84	5.57	2.28	Low	Spheroidal Surface
C18	28.66	1.83	12.86	0	Low	Spheroidal Surface
C19	11.66	1.08	12.15	1.59	Low	Vertical Plane

Here, Fisher's exact test was used to generate contingency tables for diseases and rock art locations (Table 6), as well as for diseases and rock surface types (Table 7). The resulting *p*-values were calculated and are presented in Table 8. All the calculated *p*-values for the rock art location factor exceeded the 0.05 significance level. This indicated the lack of a significant association between rock art locations and the impact of diseases in selected rock art samples.

Based on the analysis of different types of rock art surfaces, it was observed that the *p*-values for detachment (0.022) were lower than the significance threshold (0.05). This suggested a correlation between the rock art surface types and the incidence of detachment and splitting in a given sample. In particular, detachment was more likely to occur in rock art types with vertical planes and spherical surfaces.

Thus, it was observed that detachment primarily occurred on spherical-surface rock art. The elevation of rock art locations did not significantly affect the disease distribution. This suggests that surface type might be a contributing factor to detachment, which could be linked to environmental conditions and rock properties. However, further research is required to confirm these observations and investigate the mechanisms causing such diseases in Helan Mountain rock art. It is important to note that these findings are limited to the observed sample range and interpretations because of the small sample size. Other factors that might impact the occurrence of rock art diseases were not considered in this analysis. Thus, further research and data collection are necessary for a better understanding.

5.ANALYSIS OF DISEASE IMPACT BASED ON THE DAMAGE INDEX

Various methods have been investigated and developed to assess the extent of damage to rock art. One such method is the Damage Index (DI) proposed by German scientists Fitzner and Heinrichs (Randazzo L, 2020 and Fitzner B., 2004). This method has been widely employed in the graded assessment of historic European building façades and is

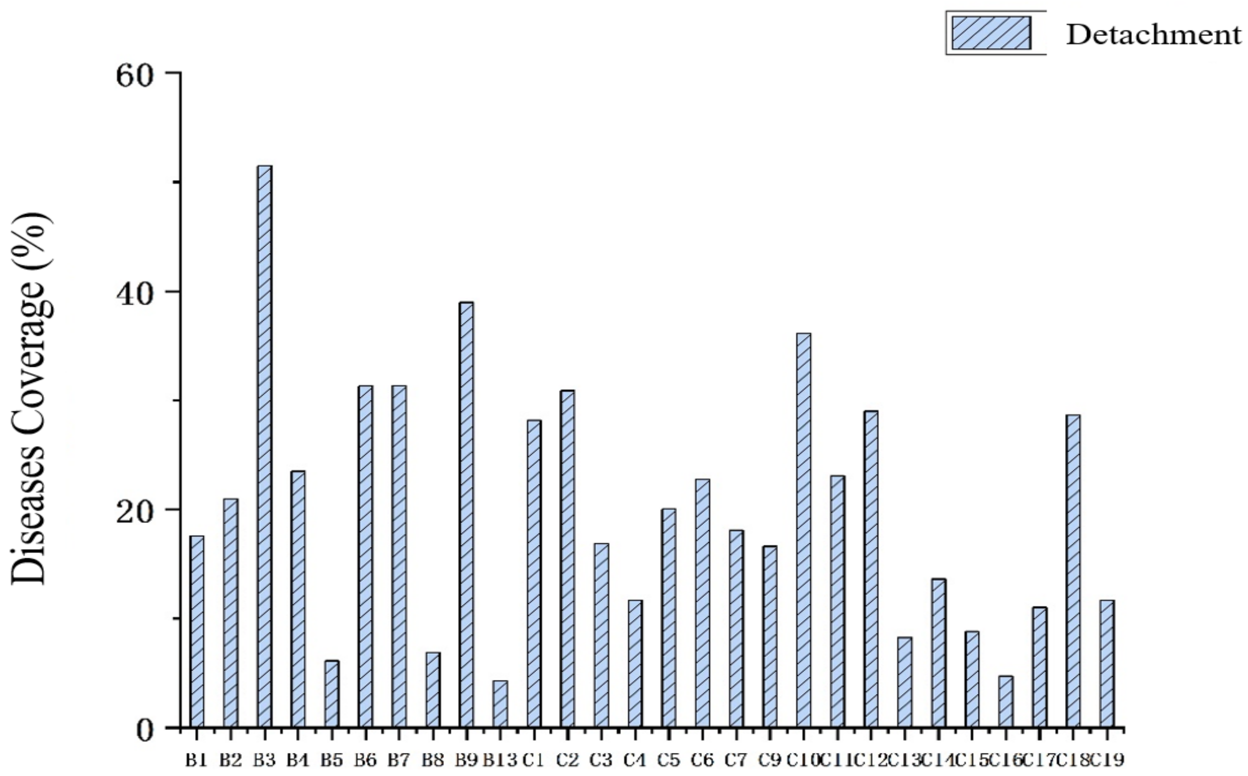

Figure 8: Detachment Disease Coverage Rate

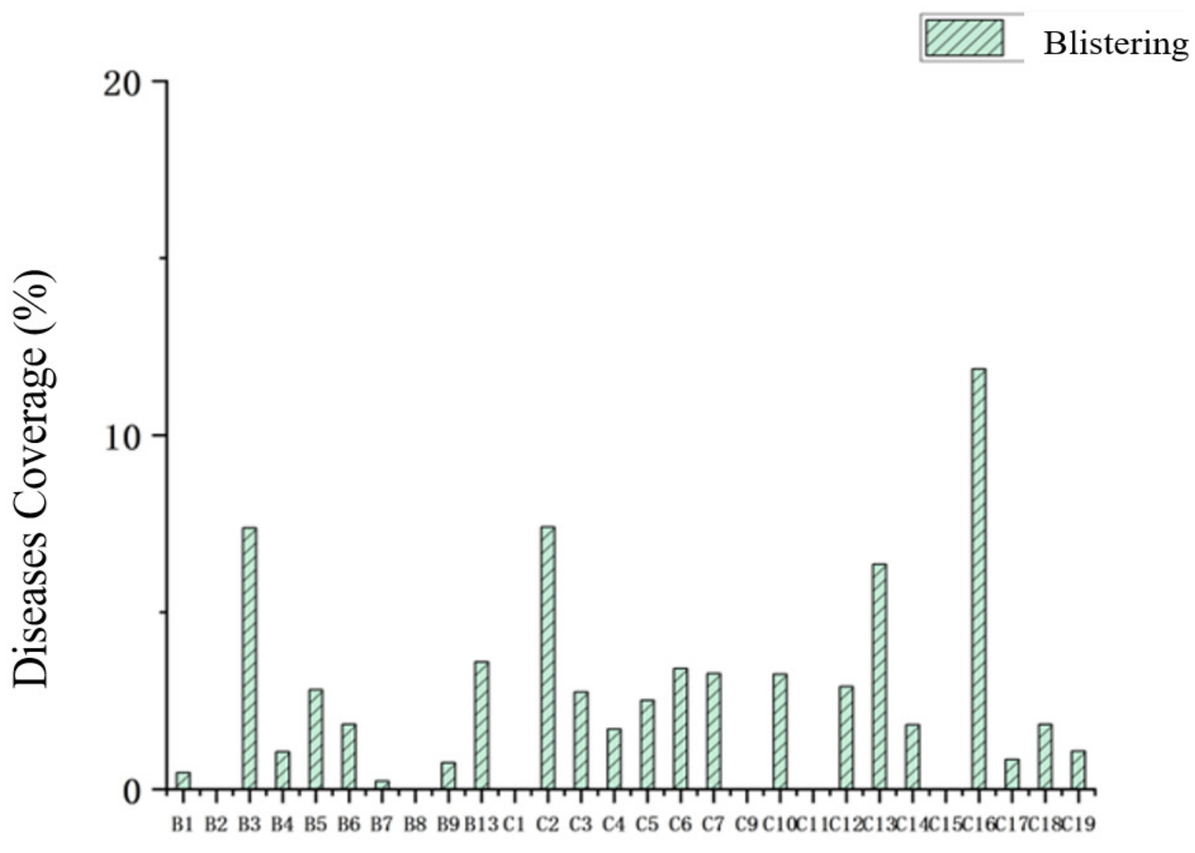

Figure 9: Blistering Disease Coverage Rate

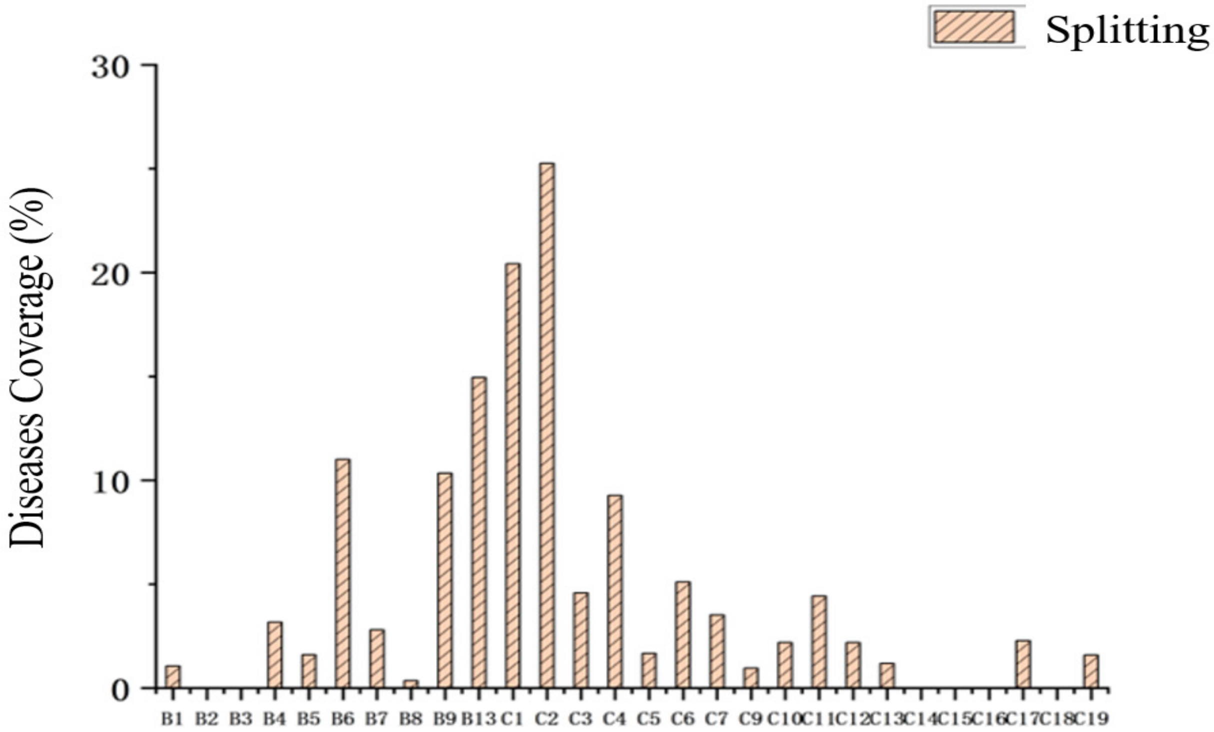

Figure 10: Splitting Disease Coverage Rate

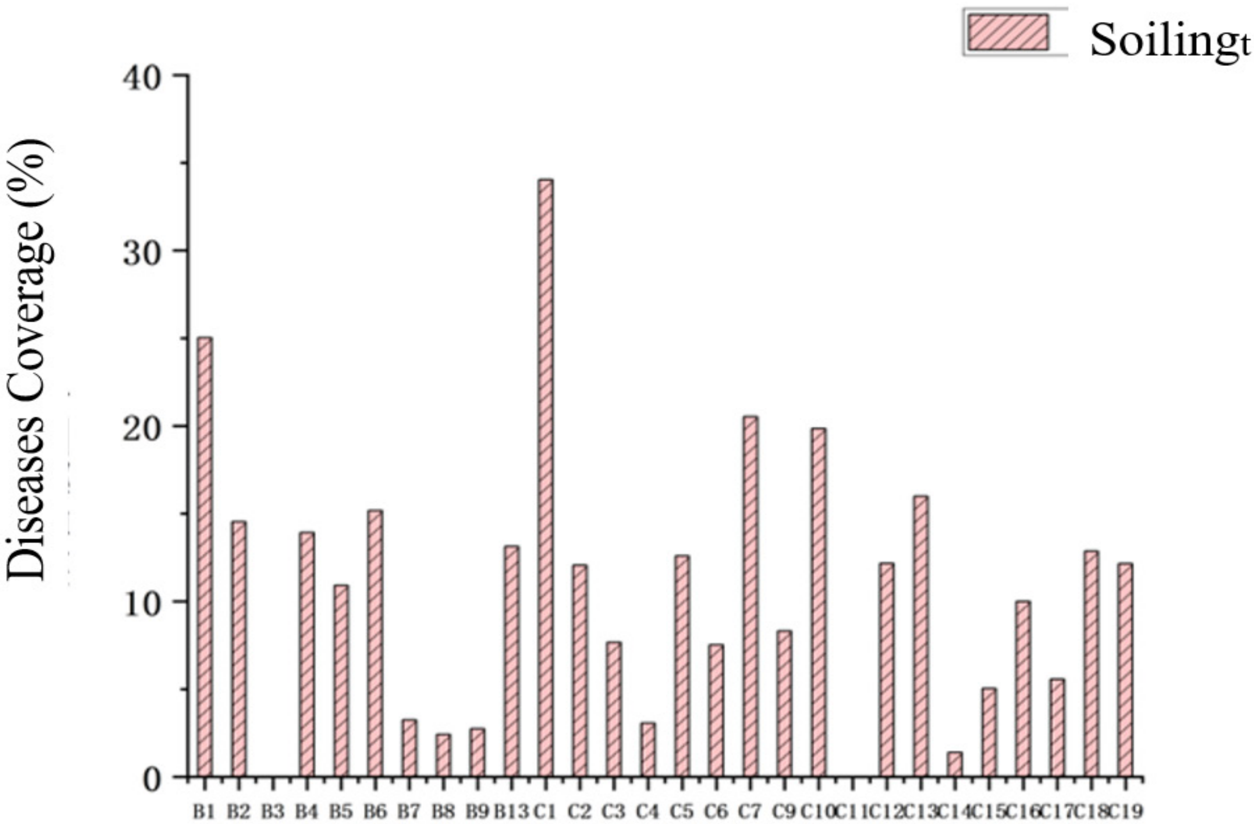

Figure 11: Soiling Disease Coverage Rate

Table 6: Cross Tabulation of Diseases and Rock Art Locations

Disease Type	Location	Disease Present	Disease Absent
Detachment	High altitude	3	8
	Low altitude	6	11
Blistering	High altitude	1	10
	Low altitude	3	14
Splitting	High altitude	5	6
	Low altitude	10	7
Soiling	High altitude	1	10
	Low altitude	3	14

Table 7: Cross Tabulation of Diseases and Rock Surface Types

Disease Type	Rock Surface Type	Disease Present	Disease Absent
Detachment	Vertical Plane	3	10
	Parallel Plane	0	5
	Spheroidal Surface	6	4
Blistering	Vertical Plane	2	11
	Parallel Plane	0	5
	Spheroidal Surface	2	8
Splitting	Vertical Plane	8	5
	Parallel Plane	2	3
	Spheroidal Surface	5	5
Soiling	Vertical Plane	4	9
	Parallel Plane	0	5
	Spheroidal Surface	0	10

Table 8: Chi-Square Test Results

Disease Type	Factor	*P*-Value
Detachment	Location	0.493
	Rock Surface Type	0.022
Blistering	Location	0.482
	Rock Surface Type	0.407
Splitting	Location	0.153
	Rock Surface Type	0.423
Soiling	Location	0.671
	Rock Surface Type	0.172

Table 9: Definition of Damage Categories

Definition	Damage Categories
No visible damage	0
Very slight damage	1
Slight damage	2
Moderate damage	3
Severe damage	4
Very severe damage	5

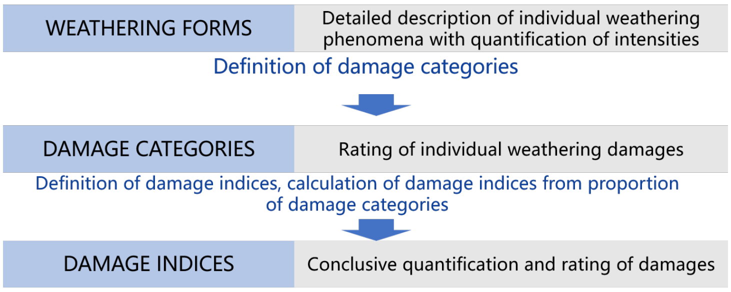

Figure 12: Damage Diagnosis

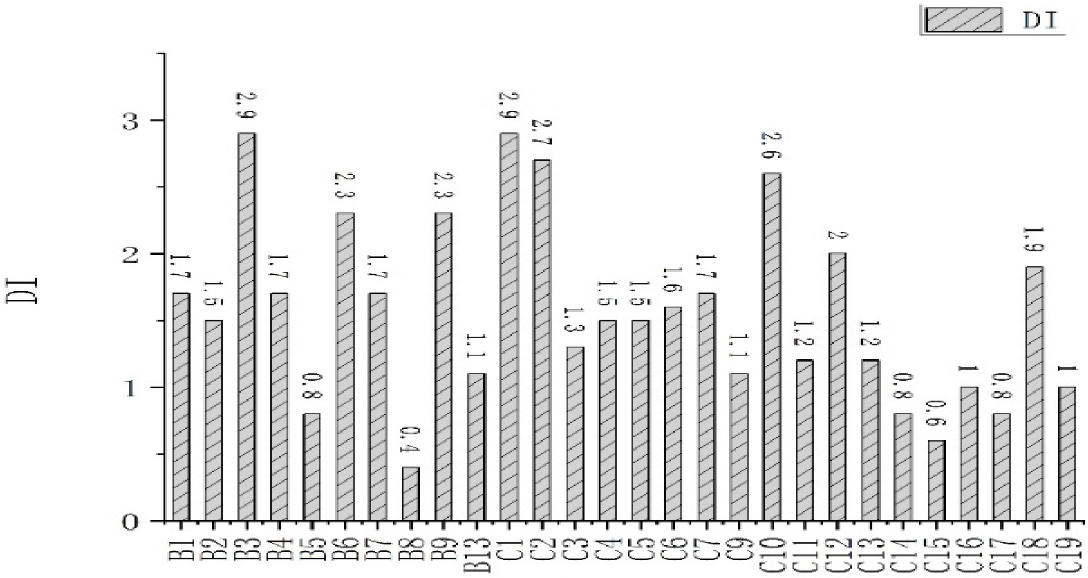

Figure 13: Detachment Disease Coverage Rate

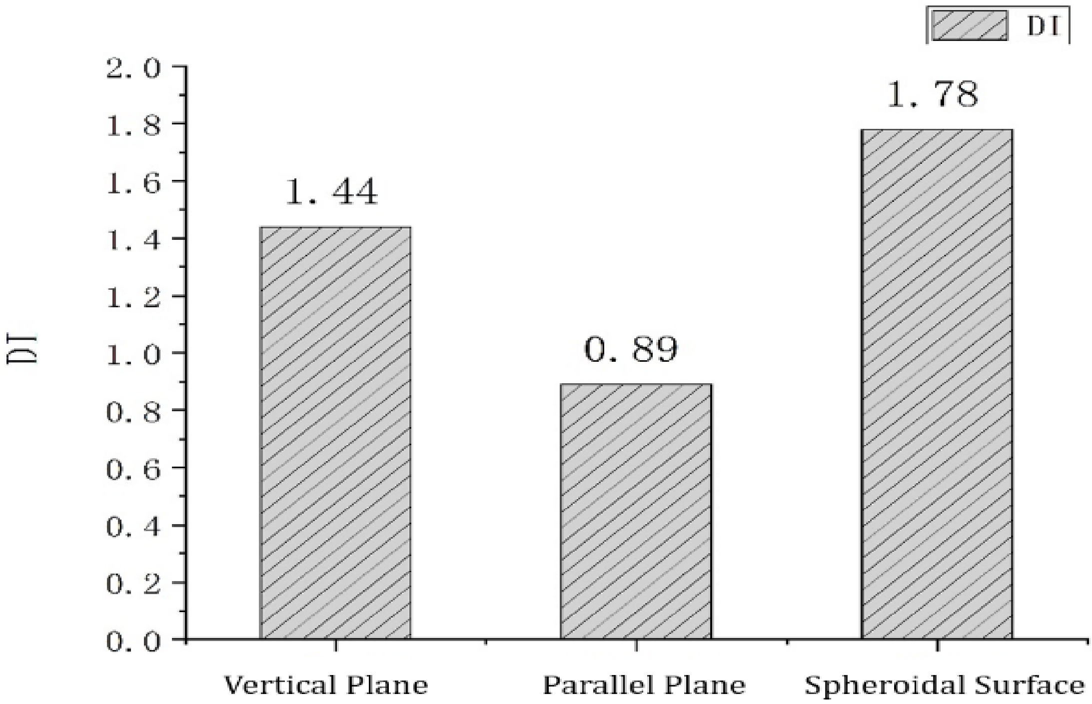

Figure 14: Blistering Disease Coverage Rate

highly suitable for the quantitative assessment of Helankou rock art diseases. The use of the DI to categorise the extent of ailment impacts on rock art in different regions and surface types provides a preliminary understanding of the necessity of protective measures for rock art. This approach offers instructive guidance for long-term investigations, maintenance, and conservation management.

The process of analysing the impact levels of diseases involves three major steps: 'weathering forms', 'damage categories', and 'damage indices' (Randazzo L, 2020) (Fig. 12). First, the damage type was determined based on the characteristic weathering ailment form of the rock art. Thereafter, the DI was calculated using the parameters of the damage type for each ailment and the proportion of the affected area (Table 9), as described in Eq. 1.

$$DI = \frac{(B\times1)+(C\times2)+(D\times3)+(E\times4)}{100}, \qquad (1)$$

The following DI assessment report describes Zones B and C (Fig. 13). This report indicates that the higher the DI, the higher the disease impact on rock art. A severe ailment impact was observed in Zones B3, C1, C2, and C10, with DI values exceeding 2.5. This indicates that these artworks were mainly affected by detachment and splitting, which call for urgent protective and therapeutic measures. A moderate ailment impact was observed in Zones B1, B2, B4, B6, B9, B13, C3, C4, C5, C6, C7, C9, C11, C12, C13, C16, C18, and C19, with DI values ranging between 1.5 and 2.5. This suggested that these artworks may have been more affected by hollowing and splitting diseases. A slight ailment impact was observed in Zones B5, B8, C14, and C15, with DI values below 1. This indicated that these artworks experienced a relatively minor ailment impact, primarily exhibiting signs of hollowing and surface pollution.

Fig. 14 shows significant differences in the severity of damage that affected the rock art on different surfaces. Artwork on vertical and spherical weathered surfaces experienced higher levels of damage, whereas those on parallel planes were relatively less affected. This difference may be related to the geological weathering process in the area and the exposure conditions in the rock art locations.

Rock art on vertical planes is frequently found in rock substrates containing dense joint systems that render the rock more permeable. Thus, these areas are more susceptible to temperature and water influence, which accelerate the weathering process of the rock and make art more prone to damage. Contrarily, spherical weathered surfaces are formed when multiple sets of joints divide a rock into polyhedral blocks. The edges and corners of these smaller rocks are initially prone to damage, which results in significant erosion. Over time, the edges of the rock gradually erode, forming spherical or ellipsoidal weathered formations. Rock art carved on spherical surfaces is more susceptible to mechanical damage, leading to overall high levels of damage.

6.CONCLUSION

This study extensively analysed the rock art of Helan Mountain and observed that rock art is affected by four primary disease types: detachment, blistering, soiling, and splitting. These diseases were unevenly distributed across regions and rock surface types, and their impact on rock art varied.

The correlation analysis between the ailment coverage rates and rock art positions revealed that the elevation of the rock art did not significantly affect ailment distribution. However, a correlation was observed between the disease coverage rates and the type of rock art surface.

After an in-depth analysis of the disease characteristics of Helankou rock art, it was discovered that the primary disease types of diseases affecting rock art included detachment, hollowing, and splitting.

Rock art with spherical and vertical surface types experienced a more pronounced impact from diseases, whereas the influence on parallel-surface rock art was comparatively less. This disparity may be due to the susceptibility of spherical and vertical surface rock art to fluctuations in environmental factors, such as temperature, humidity, sunlight exposure, rainfall, and snowfall. These findings indirectly suggest that the geological conditions affecting the existence of rock art could be some of the leading factors influencing the occurrence of ailments.

ACKNOWLEDGMENTS

The funding for this article was provided by the "Preliminary Survey Research Project on the Protection of Helankou Rock Art." We extend our sincere appreciation to the Helankou Rock Art Management Authority for their invaluable support throughout this project.

REFERENCES

He J.D., Ding Y.L., 2017. Rock Art of Helankou in Helanshan. Ningxia people's Publishing House, Pp. 1-4.

Siedel H, Siegesmund S, 2014. Characterization of Stone Deterioration on Buildings. Stone in Architecture: Properties, Durability. Berlin, Heidelberg: Springer, Pp. 349-414.

Arnold A, Jeanette D, 1979. Proposal for a terminology of weathering phenomena on building stones. Council of Monuments and Sites (ICOMOS).

Fitzner B, Heinrichs K, 1995. Weathering forms–classification and mapping. In: Snethlage R (ed) Denkmalpflege und Naturwissenschaft,

J Delgado Rodrigues, M João Revez., 2016. ICOMOS-ISCS: Illustrated glossary on stone deterioration patterns = Glossário ilustrado das formas de deterioração da pedra: XV. Paris: ICOMOS.

Li H.S.,2011, Character and Evaluation method of Historical Rock Deterioration. China University of Geosciences (Beijing), Pp. 20-32.

Zhang J.F., Li H.S.,2007, Quantitative analysis of the damage of monument and relevant evaluation software. Sciences of Conservation and Archaeology 19(3):32-36.

Fisher R A., 1922, On the Interpretation of χ2 from Contingency Tables, and the Calculation of P. Journal of the Royal Statistical Society 85(1): 87-94.

Randazzo L, Collina M, Ricca M, et al., 2020. Damage Indices and Photogrammetry for Decay Assessment of Stone-Built Cultural Heritage: The Case Study of the San Domenico Church Main Entrance Portal (South Calabria, Italy). Sustainability, 12: 5198.

Fitzner B., Heinrichs K., Bouchardiere D., 2004. The Bangudae Petroglyph in Ulsan, Korea: studies on weathering damage and risk prognosis. Environmental Geology, 46: 504-526.